Mathematical Modeling and Fluorescence Imaging to Study the Ca^{2+} Turnover in Skinned Muscle Fibers

D. Uttenweiler, C. Weber, and R. H. A. Fink
Ruprecht-Karls-Universität Heidelberg, II Institute of Physiology, D-69120 Heidelberg, Germany

ABSTRACT A mathematical model was developed for the simulation of the spatial and temporal time course of Ca^{2+} ion movement in caffeine-induced calcium transients of chemically skinned muscle fiber preparations. Our model assumes cylindrical symmetry and quantifies the radial profile of Ca^{2+} ion concentration by solving the diffusion equations for Ca^{2+} ions and various mobile buffers, and the rate equations for Ca^{2+} buffering (mobile and immobile buffers) and for the release and reuptake of Ca^{2+} ions by the sarcoplasmic reticulum (SR), with a finite-difference algorithm. The results of the model are compared with caffeine-induced spatial Ca^{2+} transients obtained from saponin skinned murine fast-twitch fibers by fluorescence photometry and imaging measurements using the ratiometric dye Fura-2. The combination of mathematical modeling and digital image analysis provides a tool for the quantitative description of the total Ca^{2+} turnover and the different contributions of all interacting processes to the overall Ca^{2+} transient in skinned muscle fibers. It should thereby strongly improve the usage of skinned fibers as quantitative assay systems for many parameters of the SR and the contractile apparatus helping also to bridge the gap to the intact muscle fiber.

INTRODUCTION

The free calcium concentration plays a central role in the contractile activation of skeletal muscle fibers. It is mainly regulated by the sarcoplasmic reticulum (SR), the intracellular Ca^{2+} ion store. The initial stages of the voltage-controlled excitation-contraction coupling (EC-coupling) are known in molecular detail (Shirokova and Rios, 1996; Melzer et al., 1995), leading to the release of Ca^{2+} ions from the SR. The regulation of the transient increase of the free myoplasmic Ca^{2+} concentration further involves the reuptake of Ca^{2+} ions by the SR Ca^{2+}-ATPase, as well as binding to various intracellular binding sites. There is still very little known about these later stages of Ca^{2+} uptake and the total Ca^{2+} turnover in the contraction-relaxation cycle under normal, diseased, or fatigued conditions and the counterion balance for neutrality (for a review see Dulhunty, 1992; Fink and Veigel, 1996; Campbell et al., 1980; Lüttgau and Stephenson, 1986).

"Skinned" muscle fibers, pioneered by Endo (1977), have proved to be very valuable preparations for studying the complex interactions determining the total Ca^{2+} turnover in muscle fibers. Skinned fiber preparations from which the outer sarcolemma has been removed mechanically (Stephenson, 1985; Fink et al., 1986; Lamb and Stephenson, 1990), chemically, or by UV-laser microdissection (Veigel et al., 1994) allow a direct diffusional access to the myoplasm with its Ca^{2+}-binding sites, while the membrane system of the SR with its release and uptake sites for Ca^{2+} ions remains fully intact. Therefore they are frequently used for studying the voltage-dependent excitation-contraction coupling in mechanically skinned fibers (e.g., Stephenson, 1985; Lamb et al., 1994), for directly examining the contractile apparatus (Fink et al., 1986; Rüegg, 1996), and for studying the sarcoplasmic reticulum in heart (Steele et al., 1996) and skeletal (Makabe et al., 1996) muscle.

In skinned fibers the regulation of the intracellular Ca^{2+} concentration by the SR can be analyzed by inducing calcium transients with a high dose of caffeine. The interpretation of the Ca^{2+} transients, measured as isometric force (Makabe et al., 1996) or a photometric fluorescence signal (Endo and Iino, 1988; Steele et al., 1996), so far has basically focused on peak amplitude values (e.g., Fink and Stephenson, 1987; Du et al., 1994) or the time integral of the force or the photometric fluorescence Ca^{2+} transients as a one-dimensional measure of Ca^{2+} release (e.g., Endo and Iino, 1988). To our knowledge, no comprehensive quantitative analysis of the total spatial and time-dependent distribution of Ca^{2+} ions in skinned fiber preparations has been carried out, because of considerable experimental problems, which mainly arise from the distribution of the fluorescent dye in the entire solution surrounding the preparation, as the sarcolemma of the fiber is permeabilized or removed. Mostly, the distinction between free Ca^{2+} ions and Ca^{2+} ions bound to various mobile or immobile buffer systems has been completely neglected.

Mathematical models have proved to be very powerful tools in studying the time course of Ca^{2+} exchange with buffer systems and the diffusional properties of Ca^{2+} ions (e.g., Gillis et al., 1982; Wagner and Keizer, 1994). For intact skeletal muscle fibers a spatially resolved model has already been developed (Cannell and Allen, 1984), demonstrating the importance of parvalbumins in the relaxation of skeletal muscles of frog and small mammals and modeling the time course of calcium gradients across a single sar-

Received for publication 12 September 1997 and in final form 11 January 1998.

Address reprint requests to Prof. Dr. Rainer H. A. Fink, Ruprecht-Karls-Universität Heidelberg, II Institute of Physiology, Im Neuenheimer Feld 326, D-69120 Heidelberg, Germany. Tel.: ++49-6221-544065 or 544084; Fax: ++49-6221-544123; E-mail: fink@novsrv1.pio1.uni-heidelberg.de.

0006-3495/98/04/1640/14 $2.00

comere (see also Caputo et al., 1997). For intact smooth muscle, the model of Kargacin (1994) presented very interesting results about intracellular Ca^{2+} concentration gradients and diffusional barriers.

However, there has been no spatially resolved model for the quantitative description of the Ca^{2+} turnover in skinned skeletal muscle fibers to date, which is desirable for further improving their usage as a quantitative assay system for many parameters of the SR and the contractile apparatus. Skinned fiber preparations assist studies on the intact physiological system, which often suffer from limited access to the myoplasm, whereas skinned fibers offer very direct access through the permeabilized sarcolemma, thus allowing to monitor physiological processes under well-defined myoplasmic conditions. Obviously one-dimensional averaged quantities (such as force or photometric fluorescence data) can give only a very crude description of the complex interplay between intrinsic and extrinsic Ca^{2+}-binding sites, Ca^{2+} transport mechanisms, and diffusion of Ca^{2+} ions in free and bound form.

The main aim of our study was to develop a combined method of mathematical modeling and fluorescence imaging for a comprehensive analysis of the total Ca^{2+} turnover in skinned muscle fibers. This approach should also improve the usage of skinned fiber preparations for the study of many parameters of the SR, and it should help to bridge the gap to the intact muscle fiber. Preliminary results have been published in abstract form (Uttenweiler et al., 1997a,b).

MATERIALS AND METHODS

Caffeine-induced Ca^{2+} transients

Single muscle fibers from the extensor digitorum longus (edl; fast twitch) of male Balb-C mice sacrificed by ether overdose were prepared in paraffin oil. The fibers were mounted in a perfusion chamber, and the sarcomere length was adjusted to 2.4 μm. The chamber was then mounted on the stage of an inverted fluorescence microscope (IMT-2; Olympus, Tokyo, Japan). The chamber is designed to have a solution flow parallel to the muscle fiber, minimizing any strain. The bottom of the chamber consists of a thin coverslip (170 μm thickness) with minimal UV absorbance (less than 10%) for fluorescence excitation wavelengths down to 340 nm. The volume of the chamber is $\sim$1 μl. The solution change is controlled via a computerized solution exchanger (List Electronics, Darmstadt, Germany), allowing solution applications as short as 10 ms. The fiber preparation is glued to a fixed hook on one end and to a force transducer (AE801; SensoNoras, Horten, Norway) at the other end with a collagen glue. All experiments were carried out at room temperature (22–23°C).

The solutions used in these experiments are prepared according to the method described by Fink et al. (1986). Total and free ion concentrations were calculated using the computer program REACT (v. 2.03, 1991, G. L. Smith, Glasgow, Scotland). Absolute binding constants were taken from Fabiato and Fabiato (1979) and Godt and Lindley (1982) and corrected for ionic strength ($\Gamma/2 = 230$ mM). All solutions were adjusted to pH 7.0 with KOH and contained 60 mM *N*-(2-hydroxyethyl)piperazine-*N*′-(2-ethanesul-phonic acid) (HEPES), 8 mM adenosine triphosphate (ATP), 10 mM creatine phosphate (CP), and 0.5 mM Mg^{2+}. The following types of solutions were used:

- High Ca^{2+}-activating solution (HA) with 50 mM ethylene glycol-bis (β-aminoethyl (ether)-*N*,*N*,*N*′,*N*′-tetra acid ions (EGTA) and 49.5 mM total Ca^{2+} (pCa 4.45).
- High relaxing solution (HR) with 50 mM EGTA (pCa 10.0).
- Low relaxing solution (LR) with 0.5 mM EGTA and 49.5 mM 1,6-diaminohexane-*N, N,N′,N′*-tetraacetic acid (HDTA) (pCa 7.99).

Solutions with various calcium concentrations were obtained by mixing appropriate amounts of HR with HA. The solution for loading the SR (LS) is a mixture of either 60% HA and 40% HR (0.6 A solution), or 65% HA and 35% HR (0.65 A). The release solution (RS) for inducing calcium release is based on the low relaxing solution containing, additionally, 30 mM caffeine and 10 μM Fura-2.

The chemical skinning of the fibers is achieved by exposing the fibers mounted in the perfusion chamber for 5 min to a LR solution containing, additionally, 50 μg/ml saponin, resulting in a selective perforation of the sarcolemma. The saponin is then washed out with a saponin-free low relaxing solution. After the skinning, the following standard experimental protocol is used for generating caffeine-induced calcium releases.

The experimental protocol starts by Ca^{2+} loading of the SR in a strongly Ca^{2+}-buffered solution (LS) at a pCa of 6.2 after exposure to the low relaxing solution (LR). After the loading, the fibers are washed with LR solution to lower the Ca^{2+} and the EGTA concentration. Calcium releases from the sarcoplasmic reticulum are induced with the release solution (RS). After the Ca^{2+} transient is recorded, the fibers are relaxed in the high relaxing solution (HR). Further releases can be obtained by subsequently repeating the experimental protocol.

Quantitative fluorescence imaging

The skinned fiber fluorescence measurements were carried out with a combined photometric and imaging system described by Uttenweiler et al. (1995). In brief, the system is based on a dual excitation photometric system (OSP-3; Olympus), in which a CCD camera (Dage 72E; Dage-MTI, Michigan City, IN) with an optically coupled image intensifier (Geniisys; Dage-MTI) and a PC-based imaging board (Image Series 640; Matrox, Dorval, Canada) were added for spatially resolved measurements.

The synchronization of the excitation wavelength changer and the image acquisition is achieved with custom-built synchronization electronics. The system allows the consecutive recording of photometric and imaging fluorescence data, with isometric force recorded simultaneously for the same muscle fiber preparation. The ratio frequency was 100 Hz for the photometric measurements and 4.17 Hz for the imaging measurements. The sample area of the photomultiplier can be selected via pinholes, which are variable in size and position (5–100 μm in diameter). We also used square openings with an area of either 50×150 μm^2 or 25×75 μm^2 in some experiments.

The fluorescence emission was recorded either with a DAPO 20×/UV/0.7 dry or with a WPLAN FL 40×/UV/0.7 (Olympus) water immersion objective. All experiments were recorded using the wavelength pair 340 nm/380 nm, and the fluorescence emission was filtered with a bandpass filter centered around 510 nm with a bandwidth of 30 nm. The Fura-2 concentration in all experiments was 10 μM, to minimize the buffering effect of the dye and to obtain a reasonable fluorescence signal.

The main problem arising in skinned fiber fluorescence experiments is the large background signal from the fluorescent dye present in the solution surrounding the fiber. In particular, the solution above and beneath the fiber makes a strong contribution to the total fluorescence signal recorded from the fiber. The chamber therefore had to be constructed to minimize this contribution, while still ensuring a homogeneous solution flow around the fiber, to yield an isotropic diffusional exchange with the bath solution.

The calibration of the fluorescence signal is achieved by using the isometric force transients recorded simultaneously with the fluorescence data. Because of the permeabilized sarcolemma standard in vitro and in vivo, calibration procedures are unsuitable for these experiments. The troponin-tropomyosin system is an indicator located entirely inside the muscle fiber, and therefore the Ca^{2+}-activated force can be used to determine the averaged free Ca^{2+} concentration inside the muscle fiber via conversion with the individually determined pCa-force relationship. The method of converting force to free Ca^{2+} concentrations has been used by Makabe et al. (1996) in skinned fiber preparations to estimate the time course of the averaged free Ca^{2+} concentration. Here we use the conver-

sion solely for the quantification of the averaged free Ca^{2+} concentration inside the muscle preparation during the recording of the spatially resolved fluorescence data (see Results).

Mathematical modeling

As skeletal muscle fibers have approximately cylindrical shape, mathematical models can exploit cylindrical geometry for an easier formulation of the equations associated with each process. All model calculations were performed assuming homogeneity along the fiber axis and radial symmetry; the experimental geometry is approximated as shown in Fig. 1. Modeling the Ca^{2+} transient leads to the solution of the diffusion equation with various sink and source terms. The diffusion equation in cylindrical coordinates, where diffusion occurs purely in the radial direction, can be written as

$$\frac{\partial c(r,t)}{\partial t} = \frac{1}{r}\frac{\partial}{\partial r}\left(rD\frac{\partial c(r,t)}{\partial r}\right) + h(r,t) \quad \text{with} \quad h(r,t) = \sum_{\ell} h_{\ell}(r,t), \tag{1}$$

where c is the concentration and D is the diffusion coefficient of the diffusing substance, r is the radial coordinate, t is the time coordinate, and $h(r, t)$ is the sum of all source and sink terms $h_\ell(r, t)$ of the various processes involved.

In the case of inward caffeine diffusion, sink and source terms can be neglected. Therefore, this situation can be solved analytically with reasonable assumptions for the boundary conditions. The subsequent Ca^{2+} transient evoked by the caffeine has to be described by the diffusion of various types of substances and by numerous sink and source terms.

Caffeine diffusion into the fiber

The initiation of the Ca^{2+} release is achieved by application of a high dose of caffeine (30 mM in our experiments) via a fast solution change of the surrounding bath solution. Let s denote the radial position of the interface between the muscle fiber and the surrounding bath solution (see Fig. 1). The caffeine diffusion into the muscle fiber is described by Eq. 1, neglecting the source and sink terms, with the boundary condition $c = c_1 = 30$ mM for $r = s$ and $t > 0$, and the initial condition $c = 0$ for $0 \le r \le s$ and $t = 0$. The solution of this problem can be obtained by the separation of variables and can be shown to be (Crank, 1975)

$$c(r,t) = c_1\left(1 - \frac{2}{s}\sum_{n=1}^{\infty} e^{-D\lambda_n^2 t}\cdot\frac{J_0(r\lambda_n)}{\lambda_n J_1(s\lambda_n)}\right), \tag{2}$$

where J_0 and J_1 are Bessel functions of zero and first order, respectively, and where the λ_n are determined by the relation $J_0(s\lambda_n) = 0$.

The graphs of Eq. 2 for different times t are shown in Fig. 2. These are calculated for a muscle fiber diameter of 60 μm, where the myoplasmic diffusion coefficient for caffeine is taken as $D = 240\ \mu m^2\ s^{-1}$ (Du et al., 1994). The infinite sum in Eq. 2 is approximated by the finite sum of the first 30 terms, which satisfies the accuracy to within 0.5%. The caffeine concentration necessary for inducing the release of Ca^{2+} ions by increasing the open probability of the Ca^{2+} channels in the SR is below 2 mM (Endo, 1977). Therefore this concentration can be taken as the lower limit necessary to initiate the Ca^{2+} release from the SR. As can be seen in Fig. 2, the caffeine concentration in the entire fiber is higher than 2 mM ($c/c_1 > 0.07$) in less than 0.3 s. The typical time scale for the rising phase of the Ca^{2+} transient in single muscle fibers with a diameter of ~60 μm is on the order of 5 s; therefore the caffeine diffusion is fast enough to justify the assumption that there is an instantaneous Ca^{2+} release within the fiber. Therefore the simulation of the Ca^{2+} transient can be carried out, neglecting the effect of retarded and spatially inhomogeneous Ca^{2+} release due to a slow caffeine diffusion into the fiber.

Numerical model of the Ca^{2+} turnover

The different components of the mathematical model describing the Ca^{2+} turnover are described in Fig. 3. The model assumes cylindrical symmetry and spatial homogeneity along the muscle fiber axis, resulting in a concentration profile depending on radius and time. The processes incorporated into the model are

1. Diffusion of free Ca^{2+} ions, Fura-2, EGTA, and the respective Ca^{2+} complexes inside the fiber and outside the fiber
2. Ca^{2+} release by the SR
3. Ca^{2+} reuptake by the SR Ca^{2+} pump

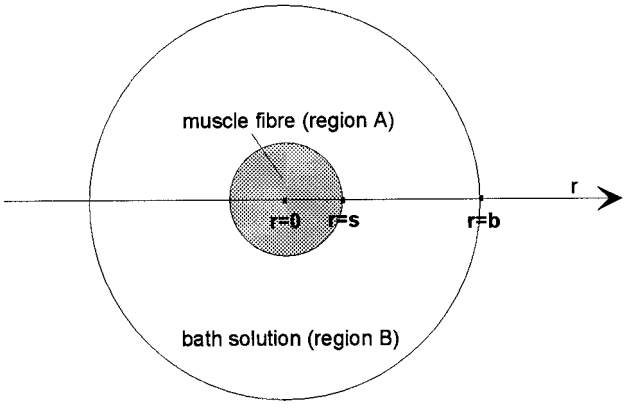

FIGURE 1 Geometry used for the mathematical modeling, approximating the experimental situation with the muscle fiber mounted in the perfusion chamber. It can be described by an infinite circular hollow cylinder, where the inner radius s corresponds to the interface between the muscle fiber (region A) and the surrounding bath solution (region B), and the outer radius b to the surface of the experimental chamber.

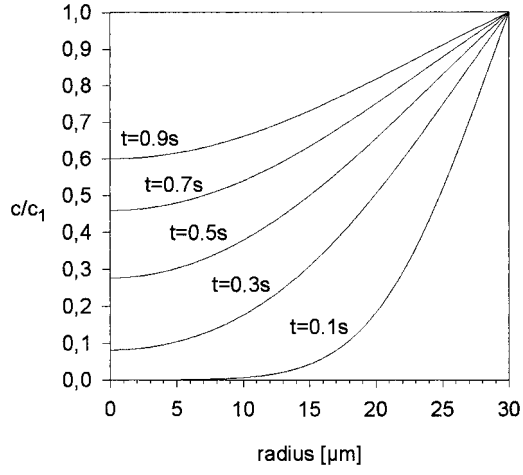

FIGURE 2 Radial caffeine concentration profiles for different times t, as obtained from model calculations, and where $t = 0$s corresponds to the application of the caffeine containing bath solution. The radius $r = 30$ μm corresponds to the muscle fiber surface, and $r = 0$ μm to the fiber center. The lower limit of the caffeine concentration necessary to open the Ca^{2+} channels is less than 2 mM, corresponding to $c/c_1 < 0.07$ for 30 mM caffeine concentration in the bath solution.

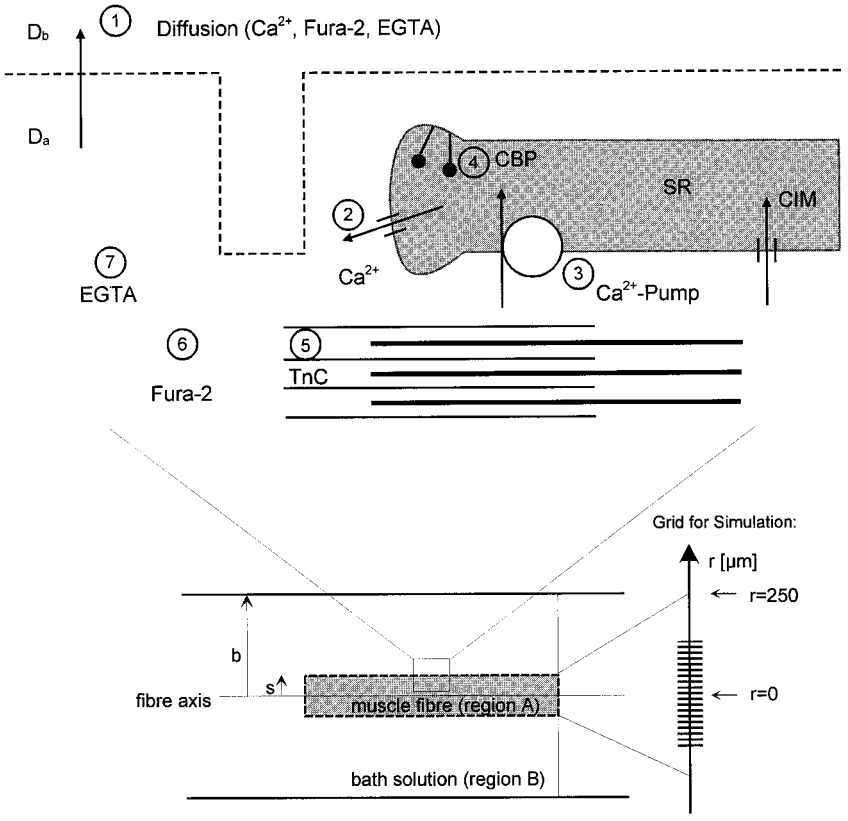

FIGURE 3 The model geometry and the components of the numerical model for the simulation of the caffeine induced calcium release in skinned muscle fibers. It includes ① the diffusion of free and bound Ca^{2+} ions as well as the diffusion of mobile buffers (EGTA, Fura-2); ② Ca^{2+} release and ③ reuptake by the SR; ④ binding to Ca^{2+}-binding proteins (CBP) inside the SR; ⑤ binding to immobile buffers (TnC) and binding to mobile buffers (⑥ Fura-2, ⑦ EGTA). Counterion movement (CIM) during SR-Ca^{2+} release is neglected in the model.

4. Binding of Ca^{2+} ions inside the SR to calcium-binding proteins (CBP), assumed to be mostly calsequestrin
5. Binding of Ca^{2+} ions to troponin-C inside the fiber
6. Binding of Ca^{2+} ions to Fura-2 inside the fiber and outside the fiber
7. Binding of Ca^{2+} ions to EGTA inside the fiber and outside the fiber

The effect of soluble Ca^{2+}-binding proteins is neglected, as the skinning leads to the washing out of these Ca^{2+} buffers (Gillis, 1985). The solution of Eq. 1 with the sink and source terms is approximated with an explicit finite-difference algorithm. The experimental situation of a muscle fiber embedded in a bath solution has to be modeled by dividing the cylindrical volume into two regions with different diffusion coefficients for each diffusing substance (compare with Fig. 1). This takes into account that the diffusion coefficients in the myoplasm are significantly smaller than in water (Allbritton et al., 1992). The geometry corresponds to that of a hollow cylinder, where the inner cylinder (region A) coincides with the muscle fiber and the outer cylinder (region B) is the bathing solution. Let $R = r/b$ and $T = Dt/b^2$ be the nondimensional radius and time, respectively, where b is the radial position of the external boundary of the system (see Fig. 1). Dividing the R-T domain into discrete intervals δR and δT, the finite-difference approximations for the diffusion term in Eq. 1, neglecting the error term, are given by (Crank, 1975)

$$c_{i,j+1} = \frac{\delta T}{2i(\delta R)^2}\{(2i+1)c_{i+1,j} - 4ic_{i,j} + (2i-1)c_{i-1,j}\} + c_{i,j} \quad \text{for} \quad i \neq 0 \qquad (3)$$

$$c_{0,j+1} = 4\frac{\delta T}{(\delta R)^2}(c_{1,j} - c_{0,j}) + c_{0,j} \quad \text{for} \quad i = 0,$$

where i denotes the radial grid position and j denotes the discrete time index.

Let s denote the subscript of the radial grid position r_s at the interface $r = s$ (cytosol for $r \leq s$ and bath solution for $r > s$). The calculation of c_S would incorporate two different diffusion coefficients, D_a, the diffusion coefficient in region A, and D_b in region B, where $D_a \neq D_b$. Therefore the interface between the two different media has to be treated separately. The conditions at the interface at $r = s$ will be dealt with by the method of "region extension," which is described by Crank (1975) for the planar case, and which we have applied to the case of purely radial diffusion in cylindrical coordinates. The explicit finite-difference formula for the calculation of c_s at the interface of region A and region B is then given by

$$c_{s,j+1} = c_{s,j} + \frac{\delta t}{\frac{s}{2s+1}\delta r_a + \frac{s}{2s-1}\delta r_b} \cdot \left[\frac{2D_a}{\delta r_a}\frac{s}{2s+1}(c_{s-1,j} - c_{s,j}) + \frac{2D_b}{\delta r_b}\frac{s}{2s-1}(c_{s+1,j} - c_{s,j})\right], \qquad (4)$$

with the further relation $\delta r_a = \delta r_b$, i.e., the grid size is equal in region A and region B.

The boundary of the system at the gridpoint representing the surface of the perfusion chamber at $r = b$ is treated with Neumann boundary conditions. This boundary condition naturally applies, as there can be no flux perpendicular to the glass surface of the perfusion chamber.

(Note: $[Ca^{2+}]$ denotes the free Ca^{2+} concentration in the following equations.)

Ca^{2+} release

The release of Ca^{2+} ions from the sarcoplasmic reticulum is assumed to be proportional to the concentration gradient across the SR membrane:

$$\frac{d[Ca^{2+}]}{dt} = k_1([Ca^{2+}]_{SR} - [Ca^{2+}]_{myoplasm}), \qquad (5)$$

where k_1 is the proportional constant, which can be used to adjust the extent of SR Ca^{2+} ion release per unit time. The finite-difference formulation for Eq. 5 is simply given by

$$h_{1\,i,j} = k_1(c_{i,j} - c^{SR}_{i,j}), \tag{6}$$

where $c^{SR}_{i,j}$ denotes the free Ca^{2+} concentration inside the SR, and $c_{i,j}$ the free myoplasmic Ca^{2+} concentration at the gridpoint (i, j).

Ca^{2+} pump

The active removal of Ca^{2+} ions from the cytosol by the SR Ca^{2+} pump is modeled with a Hill-type relation, assuming a Ca^{2+}-dependent second-order saturable pump. The uptake of Ca^{2+} ions into the SR can then be written as

$$\frac{d[Ca^{2+}]}{dt} = p \cdot \frac{v_{max}[Ca^{2+}]^n}{[Ca^{2+}]^n + K_m^n}, \tag{7}$$

where v_{max} is the maximum uptake velocity, K_m is the half-maximum uptake rate, $n = 2$ is the Hill coefficient, and p is the proportional factor. The finite-difference formula for Eq. 7 is given by

$$h_{2\,i,j} = p\,\frac{v_{max}c^2_{i,j}}{c^2_{i,j} + K^2_m}, \tag{8}$$

where $c_{i,j}$ is the free myoplasmic Ca^{2+} concentration at the gridpoint (i, j).

Kinetic description of buffer binding

Calcium is assumed to bind to all buffers in a 1:1 stochiometry and without cooperativity, so that the following equation holds:

$$\frac{d[Ca^{2+}]}{dt} = k^{\ell}_{on}[Ca^{2+}]_{free} \cdot [buffer^{\ell}]_{free} - k^{\ell}_{off} \cdot [Ca^{2+} - buffer^{\ell}], \quad \ell = 3, 4, 5 \tag{9}$$

where ℓ denotes the various buffers, k^{ℓ}_{on} is the kinetic on-rate constant, and k^{ℓ}_{off} is the kinetic off-rate constant of the buffer$^{\ell}$-Ca^{2+} binding. The finite-difference approximation is given by

$$h_{\ell_{i,j}} = k^{\ell}_{on} \cdot c_{i,j} \cdot buffer^{\ell}_{i,j} - k^{\ell}_{off} \cdot buffer^{\ell}Ca^{2+}_{i,j}, \quad \ell = 3, 4, 5 \tag{10}$$

where $buffer^{\ell}_{i,j}$ denotes the free concentration of buffer$^{\ell}$, and $buffer^{\ell}Ca_{i,j}$ denotes the concentration of the buffer$^{\ell}$-Ca^{2+} complex at gridpoint (i, j).

For the buffering of troponin-C, only the regulatory sites are considered. As the troponin concentration in skeletal muscle is ~70 μM (Gillis, 1985) and each molecule has two regulatory binding sites, as a first approximation with no cooperativity, the effective concentration can be taken as 140 μM. The high-affinity binding sites and the effect of Mg^{2+} competition are neglected in the model. The other two buffers considered are Fura-2 and EGTA.

Sarcoplasmic reticulum

For the buffering of Ca^{2+} ions inside the SR, a similar equation for kinetic buffer binding can be applied, except that the free cytosolic Ca^{2+} concentrations have to be replaced by the corresponding free SR Ca^{2+} concentrations $c^{SR}_{i,j}$. The buffering of free Ca^{2+} ions inside the SR is due to several Ca^{2+}-binding proteins (CBPs), which are present in the SR. For the numerical calculations the dissociation constant and the kinetic constants of calsequestrin were considered. Derived from the present model, the local concentration of Ca^{2+}-binding sites was assumed to be 30 mM.

In the model calculations the sarcoplasmic reticulum is treated as a separate system interacting with the myoplasm by the Ca^{2+} release and the Ca^{2+} pump term. The SR is assumed to occupy 10% of the fiber volume, and therefore the volume fraction myoplasm/SR is incorporated into the rate equations with a proportional constant.

Rate equations for concentration changes

The rate equation for the change in free myoplasmic calcium concentration at grid points inside the fiber volume is given by

$$c_{i,\,j+1} = \text{diff} + h_{1_{i,j}} - h_{2_{i,j}} - h_{3_{i,j}} - h_{4_{i,j}} - h_{5_{i,j}}, \tag{11}$$

where diff stands for the finite-difference formula described by Eq. 3 for diffusion, $h_{1i,j}$ is the Ca^{2+} release term, $h_{2i,j}$ is the Ca^{2+} pump term, $h_{3i,j}$ is the buffering of troponin-C, $h_{4i,j}$ is the buffering of EGTA, and $h_{5i,j}$ is the buffering of Fura-2. Similar rate equations can be obtained for the concentration of each substance and for the grid points outside the fiber volume. Finally, the rate equation for the free Ca^{2+} concentration inside the sarcoplasmic reticulum can be written as

$$c^{SR}_{i,\,j+1} = v_{SR} \cdot (h_{2_{i,j}} - h_{1_{i,j}}) - h_{6_{i,j}} + c^{SR}_{i,\,j}, \tag{12}$$

where $h_{6i,j}$ denotes calsequestrin buffering and $v_{SR} = 10$ is the volume factor compensating the fact that the SR occupies only 10% of the fiber volume. The changes in Ca^{2+} concentration are calculated for the myoplasm, and therefore the Ca^{2+} concentration changes inside the SR are magnified by the factor v_{SR}. Rate equations for the free and bound concentrations of calsequestrin are obtained in a similar way.

Parameters

As far as possible, the numerical values of the parameters used in the calculations were taken from published information; a summary is given in Table 1. As many of the parameters strongly depend on the experimental conditions, various parameters had to be adjusted to obtain an optimum fit between the model calculations and the experimental results. Obviously some of the parameter values had to be chosen from a broader range of published data. Where possible, we tried to choose the parameters from experimental studies that were carried out under roughly similar recording conditions, e.g., from other skinned fiber experiments. When the Ca^{2+} transients were calculated, the model proved to be most sensitive to the parameter values of the SR quantities (total amount of Ca^{2+} ions stored, properties of Ca^{2+} buffers inside the SR). It should be noted, however, that under different experimental conditions, the model is also more sensitive on other quantities, as, e.g., the diffusion coefficient for Ca^{2+}, D_{Ca}, when the extraneous buffer capacities are changed.

The resting free Ca^{2+} concentration in the fiber and the bath solution is assumed to be 25 nM. The cytosol is supposed to be in equilibrium with the surrounding LR solution at that step of the experimental protocol. The free and bound resting concentrations of the other buffers present are calculated with the knowledge of the dissociation constant for the respective buffer.

Computing

The finite-difference algorithm is programmed in ANSI-C language, and the step size for the time iteration is 14,000 time steps/s. The averaged concentration values are stored every 0.1 s, and the radial concentration data are stored every 1 s. Because of the complex nature of the calculations, they had to be carried out on UNIX Workstations (IBM-RS6000; Computing Centre, Heidelberg, Germany). The time required for calculating the various concentrations over a period of 30 s is on the order of 15 min of CPU time on the RS6000 computers.

The error in calculating the solution of the differential equations with the finite-difference algorithm was controlled by monitoring the amount of total Ca^{2+} in the model. Errors were kept below 1% in all calculations.

TABLE 1 Parameters used for simulations

Definition	Standard Value	Source
Calcium diffusion		
Cytosolic and free diffusion coefficient	$D_a = 225–300\ \mu m^2 s^{-1}$, $D_b = 700\ \mu m^2 s^{-1}$	Wagner and Keizer (1994) Cannell and Allen (1984)
Sarcoplasmic reticulum		
Resting free Ca^{2+} -concentration	$c^{SR}_{Ca\text{-}rest} = 0.5–2$ mM	Cannell and Allen (1984)
Local CS-binding site concentration	$c^{CS}_{tot} = 31$ mM	Cannell and Allen (1984)
Kinetic on- and off-rate constant CS- Ca^{2+}	$k_{on} = 8772\ M^{-1}\ s^{-1}$, $k_{off} = 10\ s^{-1}$	Donoso et al. (1995)
Dissociation constant CS-Ca^{2+}	$K_d = 1.14$ mM	Donoso et al. (1995)
SR Ca^{2+}-pump		
Maximum uptake rate	$v_{max} = 60\ \mu M s^{-1}$	Stienen et al. (1995)
Half-maximum rate	$k_m = 0.24\ \mu M$	Stienen et al. (1995)
Hill coefficient	$n = 2.07$	Stienen et al. (1995)
TnC regulatory sites		
Total local concentration	$c^{TnC} = 140\ \mu M$	Robertson et al. (1981)
Kinetic on- and off-rate constant TnC-Ca^{2+}	$k_{on} = 1.2 \times 10^8\ M^{-1}s^{-1}$, $k_{off} = 23\ s^{-1}$	Robertson et al. (1981)
Dissociation constant Ca^{2+}-TnC	$K_d = 0.2 \times 10^{-6}$ M	Robertson et al. (1981)
EGTA		
Dissociation constant EGTA-Ca^{2+}	$K_d = 0.627\ \mu M$*	Pape et al. (1995)
Kinetic on- and off-rate constant EGTA-Ca^{2+}	$k_{on} = 1.5 \times 10^6\ M^{-1}s^{-1}$, $k_{off} = 0.94\ s^{-1}$*	Pape et al. (1995)
Cytosolic and free diffusion coefficient	$D^E_b = 170\ \mu m^2 s^{-1}$, $D^{E\ =\ 340\ \mu m^2 s^{-1}}_a$	Pape et al. (1995)
Fura-2		
Dissociation constant	$K_d = 0.1–0.3\ \mu M$#	Grynkiewicz et al. (1985)
Kinetic on- and off-rate constant Ca^{2+}-Fura-2	$k_{on} = 601\ \mu M^{-1}s^{-1}$, $k_{off} = 97\ s^{-1}$	Wagner and Keizer (1994)
Cytosolic and free diffusion coefficient	$D^f_a = 50\ \mu m^2 s^{-1}$, $D^f_b = 100\ \mu m^2 s^{-1}$	Wagner and Keizer (1994)

* Strongly dependent on pH variation, value for pH 7.0.
# Dependent on ionic strength.

Radial concentration profiles and averaged quantities

The program calculates the radial concentration profiles of free Ca^{2+} ions as well as of all buffers in free and Ca^{2+}-bound form. The profiles of interest, e.g., those for free Ca^{2+} ions, Ca^{2+} ions bound to the fluorescent dye Fura-2, and Ca^{2+} ions bound to EGTA, are saved into separate files to allow their graphical representation with spreadsheet programs. Additionally averaged quantities are calculated by a quadratic averaging across the muscle fiber section, as e.g., the free Ca^{2+} concentration, the Ca^{2+}–Fura-2 concentration, and the TnC-Ca^{2+} concentration, as shown in Fig. 4. Examples of the radial concentration distribution for free Ca^{2+} ions as obtained by model calculations are also shown. The simulation is calculated for a fiber diameter of 60 μm, and the fiber center is at $r = 0\ \mu m$. Radial concentration profiles are shown for time $t = 0$ s, which corresponds to the time of caffeine application, $t = 1$ s, $t = 7$ s, and $t = 15$ s after caffeine application. The fast initial rise as well as the subsequent decline and diffusion of free Ca^{2+} ions into the surrounding bath solution can be seen.

RESULTS

Fluorescence data

The caffeine-induced Ca^{2+} transients in Fig. 5 show typical examples from 10 experiments. The Ca^{2+} transients were measured either by fluorescence imaging (Fig. 5 *a*) or by fluorescence photometry (Fig. 5 *b*). The muscle fiber in Fig. 5 *a*, with a diameter of 60 μm, is ~75% activated, as can be seen in the relative isometric force development recorded simultaneously with the fluorescence data (see Fig. 7 *a*).

The location of the muscle fiber can be seen in the bright-field image at the top left, where $r = 0\ \mu m$ corresponds to the fiber center and $r = 30\ \mu m$ to the muscle fiber surface. The first ratio image ($t = 0$ s) is recorded just before caffeine application. The homogeneous ratio reflects the fact that the fiber is in equilibrium with the surrounding bath solution. Addition of the caffeine-containing release solution (RS) leads to the release of the calcium ions from the SR into the myoplasm, which can clearly be seen in the first 2 s of the transient. After the fast initial rise inside the fiber, Ca^{2+} ions in free form and bound to the mobile buffers diffuse in the radial direction, leading to an increased fluorescence signal outside the fiber for times $t >$ 2.4 s. The overall decline of the signal after the outward calcium diffusion is visible for times $t > 6$ s. Finally, the system relaxes to a new equilibrium, with a large amount of Ca^{2+} ions bound to the various buffer systems, as can be seen in the ratio images for times $t > 15$ s.

The photometric data in Fig. 5 *b* recorded from another fiber (75 μm diameter) under similar recording conditions show the time course of the averaged Ca^{2+} concentration inside the fiber. Photometric fluorescence data were used in other publications to qualitatively estimate the time course of caffeine-induced Ca^{2+} transients (Uttenweiler et al., 1995; Steele et al., 1996). We wanted to test whether our imaging recording method with 4.17 Hz ratio frequency was fast enough to genuinely follow the time course of the Ca^{2+}-dependent fluorescence signal. It should be emphasized here that the photometric mode does not allow to quantify the total Ca^{2+} turnover in these preparations, as 1) this mode gives only very limited spatial information on the whole transient, and 2) the complex interactions of Ca^{2+} release, buffer binding, and diffusion of Ca^{2+} ions in free and bound form can only be analyzed from highly spatially

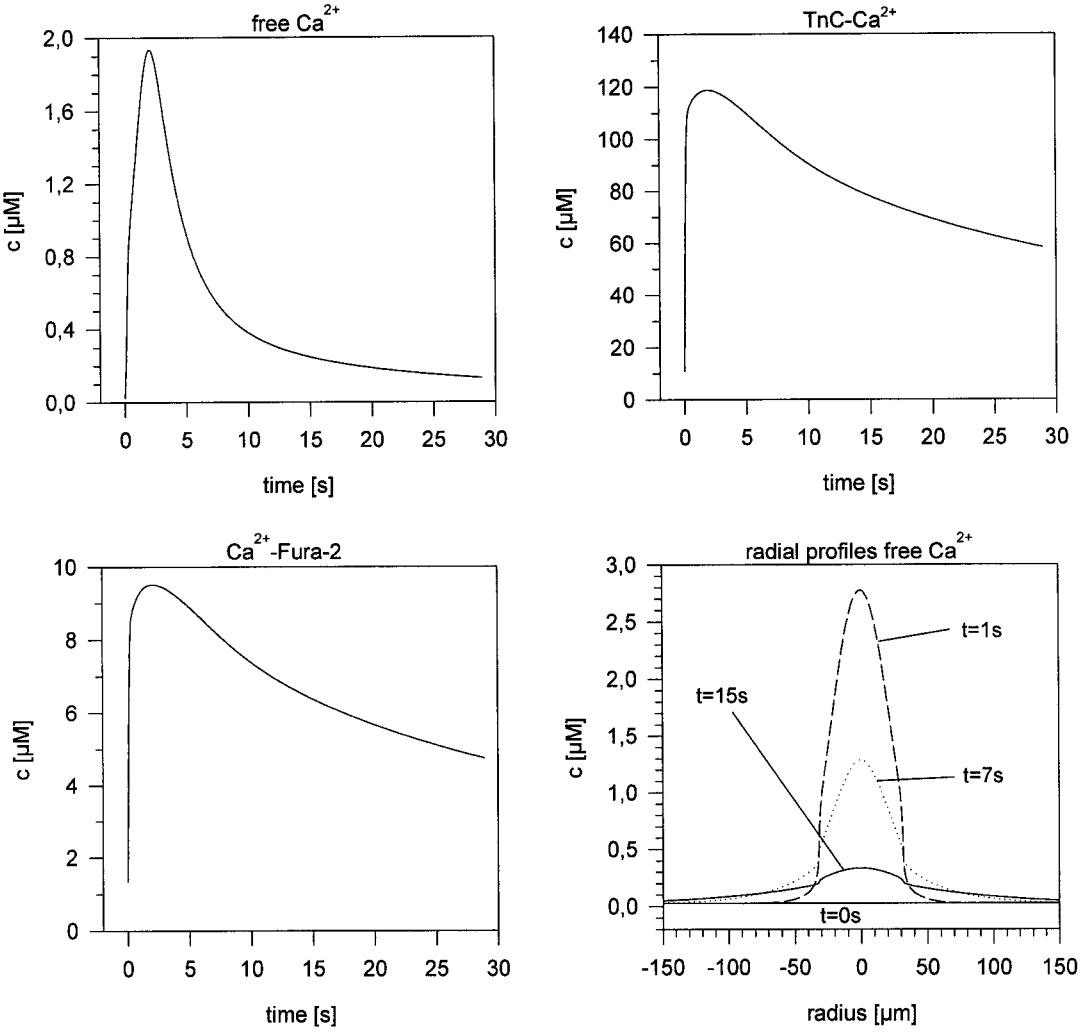

FIGURE 4 Model output for the averaged free Ca^{2+} concentration, the averaged TnC-Ca^{2+} concentration, and the averaged Ca^{2+}-Fura-2 concentration inside a muscle fiber of 60-μm diameter. The panel on the lower right side shows the calculated radial profiles of the free Ca^{2+} ion concentration at times $t = 0$ s, $t = 1$ s, $t = 7$ s, and $t = 15$ s, with the fiber located between $r = -30$ μm and $r = +30$ μm.

and temporally resolved data. Therefore, the detailed analysis of the Ca^{2+} transient must include the quantification of the Ca^{2+} ion distribution in the entire extension of the experimental chamber with the imaging method. We compared the photometric recording taken with a ratio frequency of 100 Hz with the imaging data obtained by integrating the ratio values of each image across the same area as the pinhole was set in the photometric mode. Fig. 5 *b* shows that the time courses given by the two sets of data are very similar, when we take into account a small rundown seen in the imaging mode, and that the temporal resolution of the imaging data is sufficient to follow the Ca^{2+} transient in time.

Radial concentration profiles

To specify the radial calcium concentration profile, intensity cuts perpendicular to the muscle fiber axis were obtained from each ratio image of the time series shown in Fig. 5. Aligning these intensity cuts in time results in the radial concentration profile displayed in Fig. 6. When using the ratiometric fluorescence dye Fura-2, the ratio signal is independent of the specimen thickness (Grynkiewicz et al., 1985; Uttenweiler et al., 1995), and therefore any change in ratio is directly correlated with a change in calcium ion concentration bound to the fluorescent dye.

The profiles in Fig. 6 show the typical characteristic of a skinned fiber Ca^{2+} transient, where $r = 0$ μm represents the center of the muscle fiber, and $r = 30$ μm represents the interface between the fiber and the surrounding bath solution.

The fast initial rise of the Ca^{2+} concentration inside the fiber is reflected by the steep ratio increase between $r = 0$ μm and $r = 30$ μm in the first 3 s. The subsequent diffusion of Ca^{2+} ions into the surrounding bath solution is indicated by the increased ratio signal for $r > 30$ μm. The final

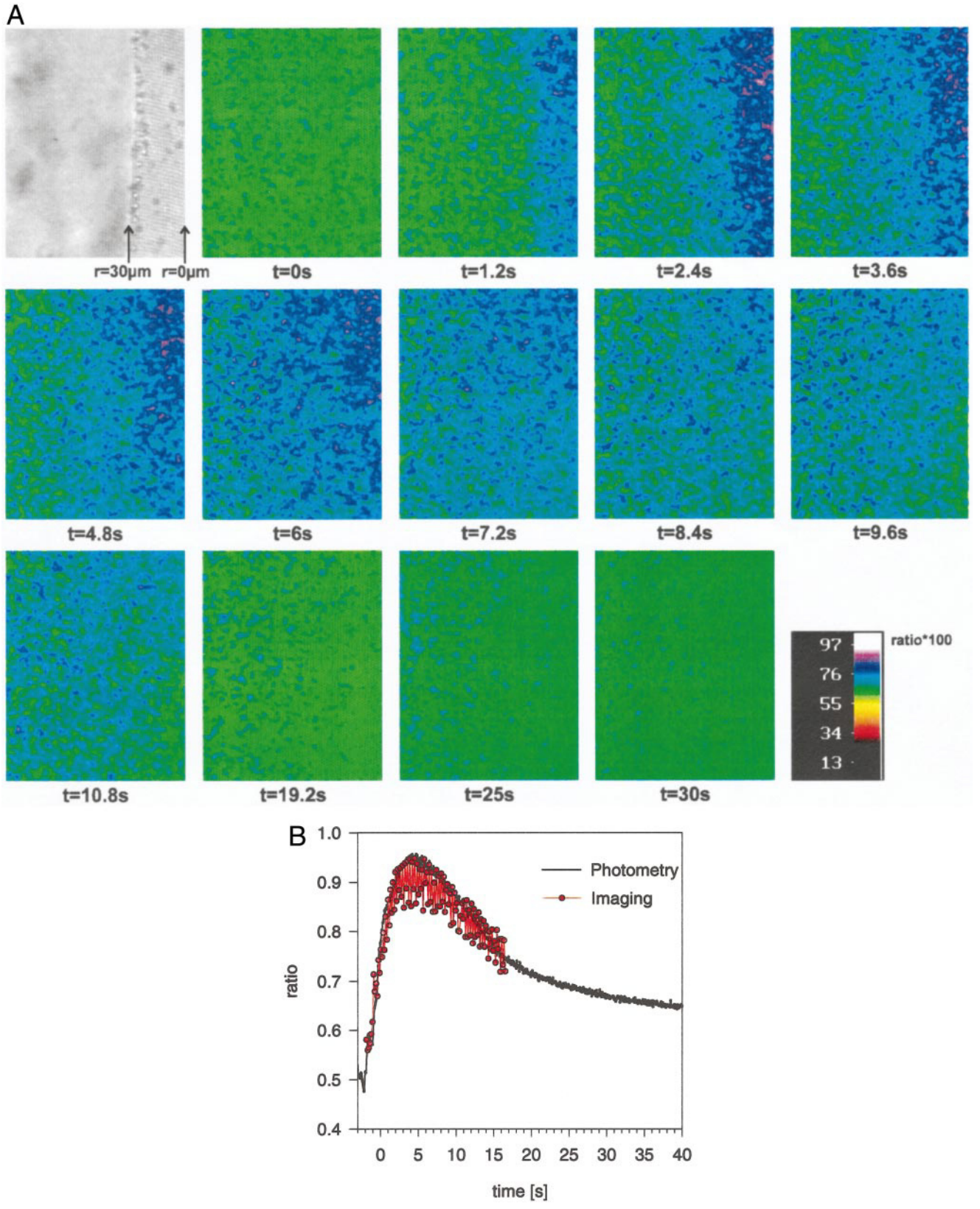

FIGURE 5 (*a*) Selected ratio images of a caffeine-induced Ca^{2+} transient in a single skinned muscle fiber, acquired with a ratio frequency of 4.17 Hz. The location of the fiber, with a diameter of 60 μm, can be seen in the brightfield image at the top left, where $r = 0$ μm corresponds to the fiber center, and $r = 30$ μm to the muscle fiber surface. The ratio images, selected from the full time series, visualize the diffusional properties of skinned fiber preparations. (*b*) A photometric Fura-2 Ca^{2+} transient recorded from a preparation with 75 μm diameter shows the time course of the averaged Ca^{2+} signal inside the fiber. The dots correspond to averaged imaging data of this preparation, obtained by integrating the ratio values of each image across the same area as the pinhole was set in the photometric mode.

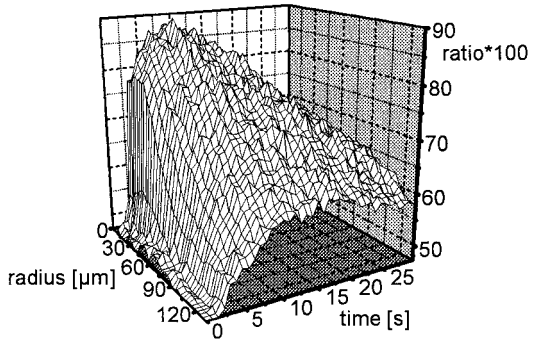

FIGURE 6 The radial distribution of the ratio fluorescence signal as obtained from intensity cuts perpendicular to the muscle fiber axis of each ratio image of the time series in Fig. 5 *a*. Aligning these intensity cuts along the time axis leads to the graph, which consequently reflects the temporal change in the Ca^{2+} ion profile. The muscle fiber center is at $r = 0$ μm, and the surface is at $r = 30$ μm.

decline of the signal, reaching equilibrium with the highly saturated buffers, is reflected by the constant radial value of the ratio for times $t > 15$ s.

Comparison of experimental and simulated data

Further analysis of the time series is accomplished by comparison of the experimental data with the output of the model calculations. The isometric force transient in Fig. 7 *a*, recorded simultaneously with the fluorescence data in Fig. 5 *a*, can be converted to the mean free Ca^{2+} transient shown in Fig. 7 *c* with the help of the individually determined pCa force relation (Fig. 7 *b*), as described in Materials and Methods. Therefore quantitative information about the time course of the averaged free Ca^{2+} concentration inside the muscle fiber is available for each experiment. The same quantity is obtained from the model calculations, and therefore both time courses can be fitted to result in the calibration of the model output. The modeled free Ca^{2+} concentration was fitted to the experimental data to yield the minimum difference in time to peak and peak height of the free Ca^{2+} ion transient, as also shown in Fig. 7 *c*.

The parameters for fitting the curves were cytosolic Ca^{2+} diffusion coefficient ($D_a = 350$ $\mu m^2 s^{-1}$), resting free Ca^{2+} concentration in the lumen of the SR ($c^{SR}_{Ca\text{-}rest} = 1.2$ mM), the dissociation constant for Fura-2 ($K_d = 0.161$ μM), and the proportional constant ($k_1 = 0.8$). The various radial concentration profiles obtained from the model calculations are shown in Fig. 8. It is apparent that the radial concentration profile for free Ca^{2+} ions is markedly different from the radial concentration profile of the Ca^{2+}–Fura-2 complex and from the radial concentration profile of the total Ca^{2+} concentration. The free Ca^{2+} ion distribution possesses pronounced local gradients not anticipated from the measured Fura-2 ratio profile without this further analysis. The origin of these increased gradients lies in the complex interactions of the various buffer systems in the cellular environment and the nonlinearity of the dependence of the ratio from the free Ca^{2+} concentration.

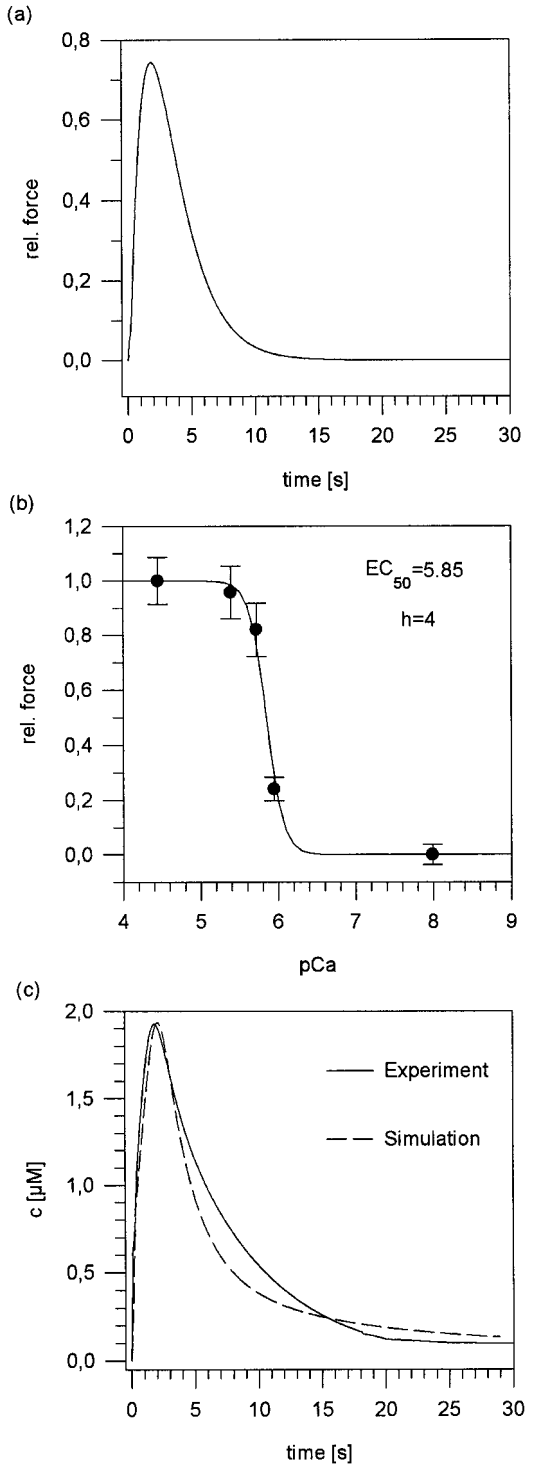

FIGURE 7 The isometric force transient in *a* was recorded simultaneously with the imaging data of Fig. 5 *a*. With the help of the individually determined pCa force relation (*b*), it can be converted to the mean free Ca^{2+} transient (*c*). In *c* the modeled free Ca^{2+} concentration as fitted to the experimental time course is additionally displayed.

The total Ca^{2+} ion concentration is mainly influenced by the concentration of Ca^{2+} ions bound to the main buffer EGTA. This is shown in Fig. 8, in which the radial concentration profile of the total Ca^{2+} concentration closely fol-

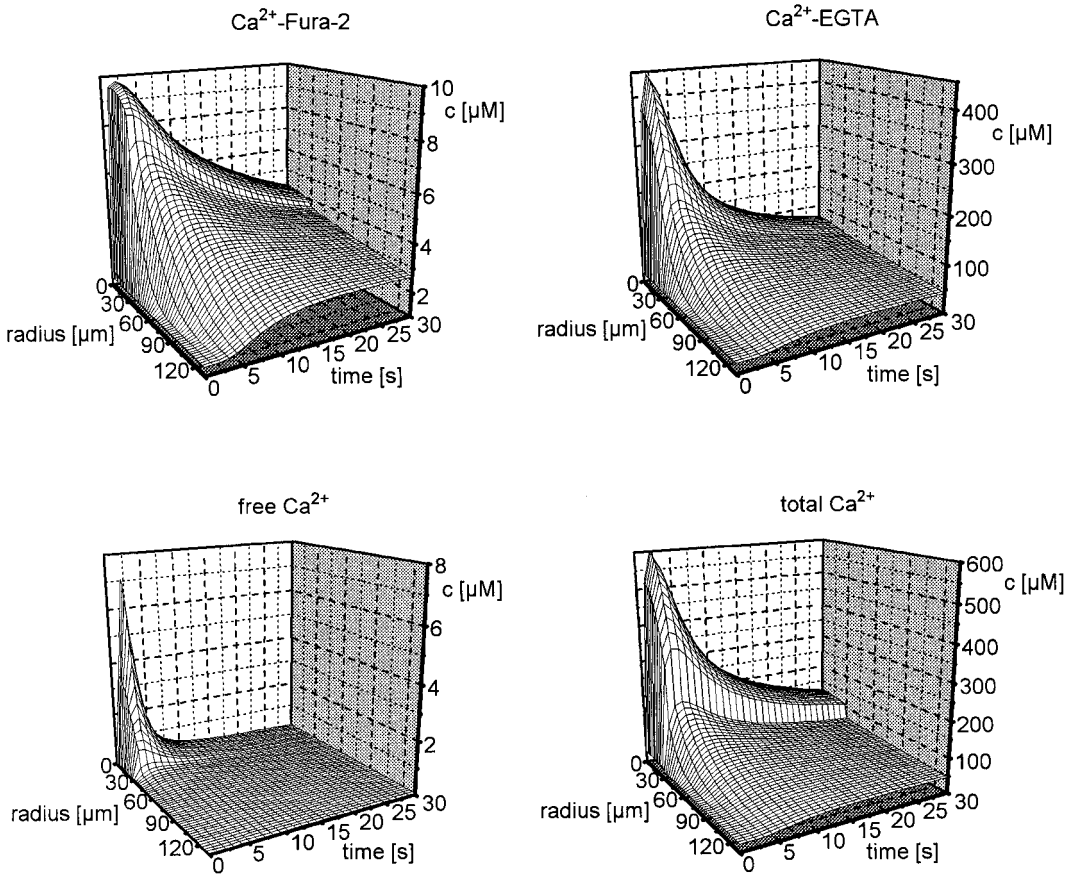

FIGURE 8 The spatial and temporal distribution of the free Ca^{2+} ion concentration, the Ca^{2+}–Fura-2 concentration, and the Ca^{2+}-EGTA concentration as modeled for a single muscle fiber with a diameter of 60 μm. In addition, the spatiotemporal course of the total Ca^{2+} ion concentration is reconstructed in the lower right panel. Again, $r = 0$ μm denotes the fiber center and $r = 30$ μm the muscle fiber surface.

lows the radial concentration profile of the Ca^{2+}-EGTA complex. The largest deviation is found in the region of the fiber (from $r = 0$ μm to $r = 30$ μm in Fig. 8), where a significant amount of the total Ca^{2+} ion concentration originates from Ca^{2+} ions bound to the troponin C system. It should be noted that fewer than 5% of the total Ca^{2+} ions in the cytoplasm seem to be present as free Ca^{2+} ions, in agreement with Smith et al. (1996).

The relative contributions of the various Ca^{2+} concentrations to the total Ca^{2+} ion concentration inside the fiber are displayed in Fig. 9. During the fast initial rise, the relative contribution of the Ca^{2+}-EGTA complex decreases briefly and the Ca^{2+}-troponin contribution is dominant (Fig. 9 *a*). This reflects the fact that EGTA is a slow buffer compared to troponin ($K_{on} = 1.5 \times 10^6$ M^{-1} s^{-1} for EGTA and $K_{on} = 1.2 \times 10^8$ M^{-1} s^{-1} for TnC). After 1 s, over 60% of the Ca^{2+} ions are bound to EGTA, which now acts as the main buffer in the system. The time course of the relative contribution of free Ca^{2+} ions inside the fiber is shown in Fig 9 *b* and indicates that fewer than 0.5% of the Ca^{2+} ions inside the fiber are in free form, even during peak release.

Examples of other quantities of interest that can easily be extracted from the model calculations are shown in Fig. 10. The release flux of Ca^{2+} ions from the SR and the time course of the free Ca^{2+} ion concentration inside the lumen of the SR are given in Fig. 10, *a* and *b*, respectively. Fig. 10 *c* shows the time course of the total flux of Ca^{2+} ions across the permeabilized sarcolemma from the fiber preparation into the bath solution. It should be noted that the peak flux is reached at time $t = 1.65$ s, in comparison to the peak free Ca^{2+} concentration at time $t = 2.35$ s (compare with Fig. 7 *c*). This implies that the relaxation phase of the transient is not linearly correlated with the outward diffusion of Ca^{2+} ions through the sarcolemma, but is the result of the complex interplay of active Ca^{2+} reuptake by the SR, diffusional, and buffer binding processes. Finally, Fig. 10 *d* shows the rate of change in free Ca^{2+} concentration inside the fiber preparation derived from the modeled free Ca^{2+} transient in Fig. 7 *c*.

In principle, the model allows the extraction of every quantity that is explicitly or implicitly present in the model, thus providing a powerful tool for analyzing all kinds of relevant quantities.

DISCUSSION

The importance of skinned fiber preparations in analyzing many functions of muscle fibers implies the need for a

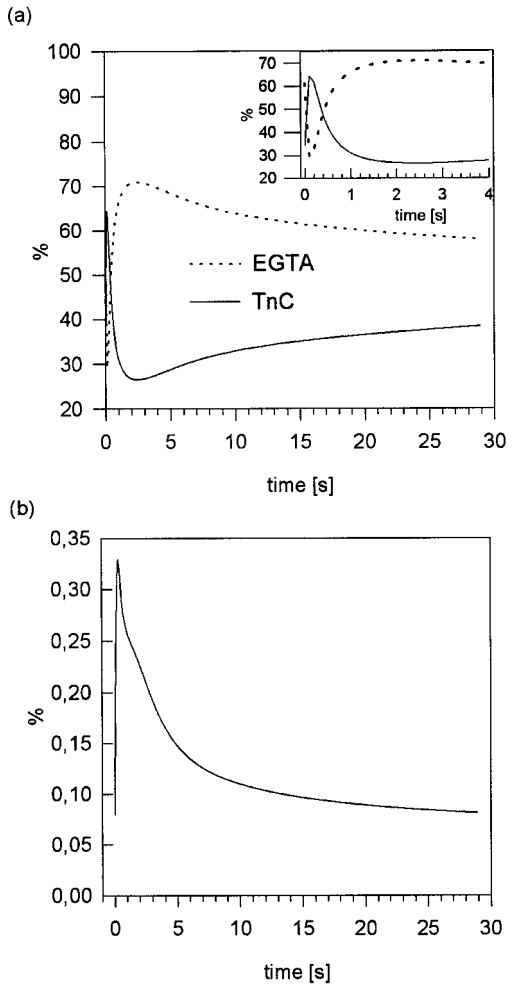

FIGURE 9 Percentage of the different contributions to the total Ca^{2+} ion concentration inside the muscle fiber during the caffeine-induced calcium release. (*a*) Relative contribution of the two main buffer systems EGTA and TnC inside the muscle fiber. The inset is an enlarged view of the first 4 s. (*b*) Contribution of free Ca^{2+} ions to the total Ca^{2+} ion concentration inside the muscle fiber.

general characterization of the main properties of these preparations. In particular, the analysis of the Ca^{2+} regulation mechanism of the sarcoplasmic reticulum in heart (Steele et al., 1996) and skeletal (Makabe et al., 1996) muscles, using skinned fiber preparations, requires a detailed understanding of the caffeine-induced Ca^{2+} transients used for this purpose. The concentration distribution of Ca^{2+} ions, in bound and free form, is necessary for the exact interpretation of experimental findings, e.g., when analyzing changes of Ca^{2+} regulation in muscle preparations from transgenic animals or when studying the contribution of single processes to the overall Ca^{2+} turnover.

First it should be noted that the time scale for the rising phase of contractile force development in caffeine-induced Ca^{2+} releases in skinned fiber preparations is not correlated with the diffusional delay of caffeine entering the muscle fiber. As shown in Fig. 2, the threshold concentration for Ca^{2+} release is reached in less than 300 ms for 30 mM external caffeine concentration and a muscle fiber preparation with 60 μm diameter. The time to peak of force development and also in free Ca^{2+} concentration is on the order of 3–5 s. This slow response is an intrinsic feature of the complex interaction of the permanent release of Ca^{2+} ions, diffusion, and subsequent buffer binding of Ca^{2+} ions in these preparations, even when assuming instantaneous Ca^{2+} release within the entire fiber, as in the numerical simulations. In thicker preparations, additional diffusional delay may occur, leading to a further prolongation of the rising phase.

The present results indicate that the free Ca^{2+} ion distribution during caffeine-induced Ca^{2+} transients is markedly different from the distribution one would expect from a less detailed analysis of fluorescence measurements alone. The complex interaction of the various processes involved in the Ca^{2+} transient leads to a highly nonuniform distribution of Ca^{2+} ions between the different buffer systems and the free form of Ca^{2+} ions.

The basic properties of caffeine-induced calcium transients in skinned skeletal muscle fibers can be described by the following processes. Ca^{2+} ions partially bound inside the SR by calcium-binding proteins with the main properties of calsequestrin are released into the myoplasm. The release is proportional to the free Ca^{2+} ion gradient across the membrane of the SR. The Ca^{2+} ions subsequently bind to the stationary buffer troponin C, leading to the development of isometric force. The pump mechanism of the SR Ca^{2+}-ATPase, described by a sigmoidal Hill-type function, actively removes Ca^{2+} ions from the cytosol and leads to a partial reloading of the sarcoplasmic reticulum. The Ca^{2+} ions that bind to the mobile buffers EGTA and Fura-2 additionally undergo diffusional translocation, as do the free Ca^{2+} ions. The diffusion of Ca^{2+} ions out of the fiber is directly visualized in the imaging data of Fig. 5.

The results of the numerical simulations reveal that the concentration gradients for the free Ca^{2+} concentration are very steep. The fact that less than 0.5% of the averaged Ca^{2+} ion concentration inside the fiber is in free form, which is even smaller than in intact cellular preparations (Smith et al., 1996), might come from the high extraneous buffer capacity of EGTA, which, in summary, increases the total buffer capacity, although soluble Ca^{2+}-binding proteins are washed out.

The fact that intracellular gradients in free Ca^{2+} concentrations are much higher than estimated from nonspatially resolved photometric measurements alone has very recently been discussed by Smith et al. (1996). Often intracellular free Ca^{2+} gradients are underestimated. For example, recording the fluorescence signal from intact muscle preparations with extended axial dimensions generally leads to a reduction of the apparent size of any concentration gradients (Duty and Allen, 1994). In skinned fiber experiments, the experimental data are even more difficult to interpret, as the recorded fluorescence signal additionally contains contributions from areas above and beneath the fiber. The difficulty of an extended depth of focus is also inherent in the fact that

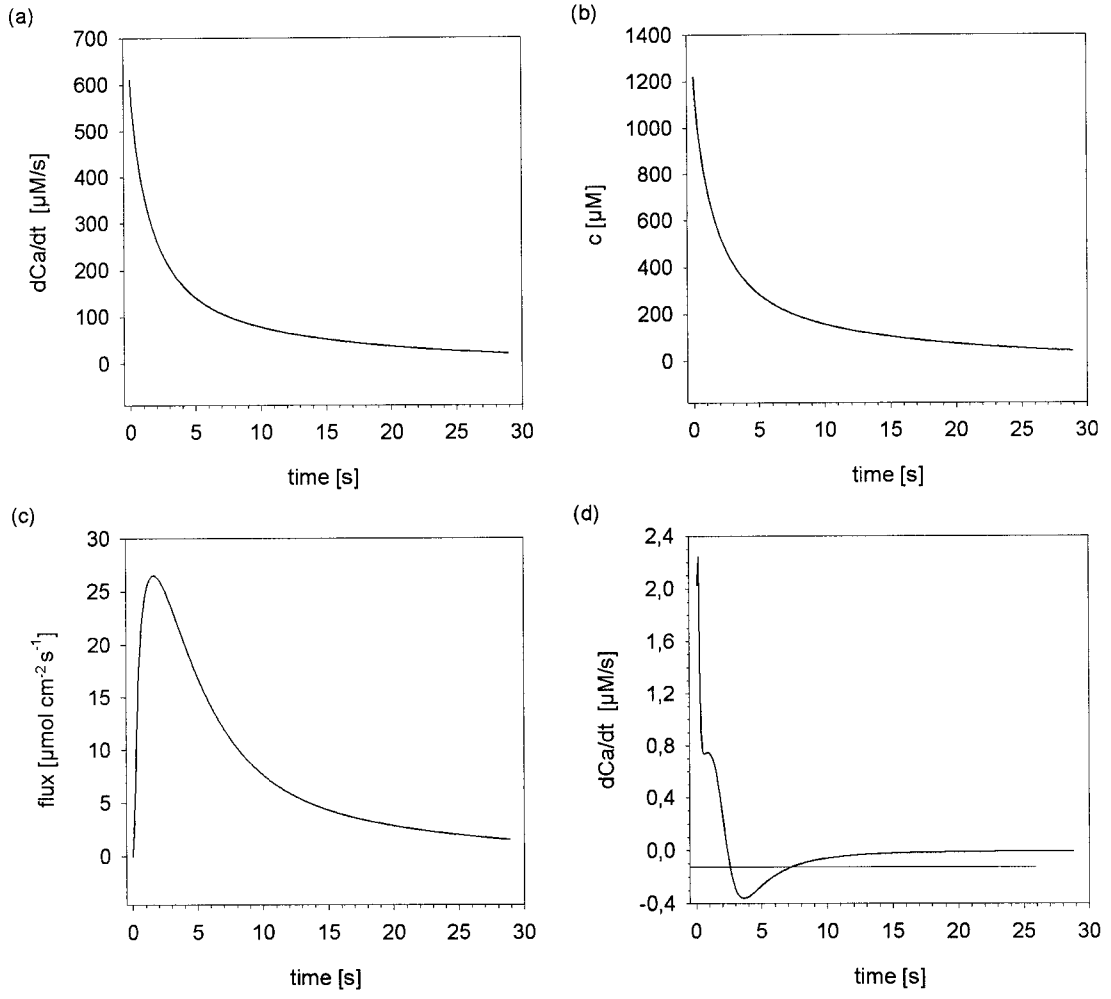

FIGURE 10 (*a*) Time course of the release rate of Ca^{2+} ions from the sarcoplasmic reticulum. (*b*) Time course of the free Ca^{2+} ion concentration inside the sarcoplasmic reticulum. (*c*) Flux of Ca^{2+} ions across the permeabilized sarcolemma from the fiber preparation into the surrounding bath solution. (*d*) Time course of the rate of change in free Ca^{2+} ion concentration inside the fiber preparation derived from the modeled free Ca^{2+} transient in Fig. 7 *c*.

diffusion in the axial direction (*z* axis of the optical system) cannot be resolved with the present setup. This is the reason for the apparent delay in time to peak for the Fura-2 signal (t_{max} = 3 s for the Fura-2 transient in Fig. 5 *a*) in comparison to the isometric force (t_{max} = 2 s for the isometric force transient in Fig. 7 *a*). The same behavior can be detected when analyzing the time to peak for the measured Fura-2 signal in Fig. 6 and the calculated time course of the Ca^{2+}–Fura-2 concentration in Fig. 8. Confocal measurements in the central plane of the muscle fiber would possibly allow measurements avoiding artefacts due to out-of-focus information and extended depth of focus. But these measurements, when typically performed with the Ca^{2+} indicator Fluo-3 excited with an argon ion laser at λ = 488 nm, would also suffer from a weak *S*/*N* ratio due to the high inner filter effect of Fluo-3.

Other sources of error in determining intracellular concentration gradients with fluorescence indicators originate from the binding of the fluorescent dye to intracellular binding sites. Fura-2 is known to bind to various cell constituents (Zhao et al., 1996), subsequently altering its kinetic on- and off-rate constants for Ca^{2+} binding. The binding also reduces the diffusional translocation of the dye. Because the changes in the dye properties have not yet been quantified, it is difficult to predict their effect on the current measurements. Furthermore, the locally high Ca^{2+} concentrations may lead to local saturation of the dye.

The spatially resolved model allows incorporation of new findings, e.g., pharmacological effects or the effects of H^+ and Mg^{2+} ions, which compete for different Ca^{2+}-binding sites of proteins involved in EC coupling or of Ca^{2+} buffers. A more realistic geometry of the sarcoplasmic reticulum with an extension of the model into a full three-dimensional description is also planned, for a more detailed spatial analysis. Furthermore, we want to include possible effects of counterion movements during release and reuptake of Ca^{2+} ions. These counterion movements are thought to shunt the SR membrane potential (for a review see Fink and Veigel, 1996).

In summary, our method allows the detailed analysis of the spatial and time-dependent Ca^{2+} turnover in skinned fiber preparations. The knowledge of the complex interac-

tions resulting in the macroscopic Ca^{2+} transient is essential when physiologically relevant effects have to be inferred from the isolated properties of the components involved (e.g., SR Ca^{2+}-ATPase).

Thus the combination of mathematical modeling and digital image analysis will allow to make selective tests of the most important parameters contributing to the Ca^{2+} turnover in skinned muscle fibers by making careful changes in the experimental conditions, e.g., by making changes in the buffer capacities of the solutions that mimic the myoplasm, or selectively blocking the SR-ATPase. It will be a major future aim to address physiologically important questions of Ca^{2+} regulation with the combined tools of mathematical modeling and fluorescence imaging. This approach should greatly help to bridge the gap between the intact physiological muscle cell and the skinned muscle fiber preparation. From our study it will now be possible to directly link our skinned fiber data to similar mathematical models of intact fibers. It may also be valuable for a variety of other permeabilized cellular and subcellular preparations.

This work was supported by grants from the Ministerium für Wissenschaft und Forschung Baden-Württemberg and the European Community (BMH4-CT96 1552).

REFERENCES

Allbritton, N. L., T. Meyer, and L. Stryer. 1992. Range of messenger action of calcium ion and inositol 1,4,5-triphosphate. *Science.* 258:1812–1815.

Campbell, K. P., C. Franzini-Armstrong, and C. E. Shamoo. 1980. Further characterisation of light and heavy sarcoplasmic reticulum vesicles. *Biochim. Biophys. Acta.* 602:97–116.

Cannell, M. B., and D. G. Allen. 1984. Model of calcium movement during activation in the sarcomere of frog skeletal muscle. *Biophys. J.* 45: 913–925.

Caputo, C., P. Bolanos, and A. L. Escobar. 1997. Fast calcium clearance by parvalbumin during single twitches in skeletal muscle fibres. *Biophys. J.* 72:A274.

Crank, J. 1975. The Mathematics of Diffusion. Oxford University Press.

Donoso, P., H. Prieto, and C. Hidalgo. 1995. Luminal calcium regulates calcium release in triads isolated from frog and rabbit skeletal muscle. *Biophys. J.* 68:507–515.

Du, G. G., C. C. Ashley, and T. J. Lea. 1994. Effects of thapsigargin and cyclopiazonic acid on the sarcoplasmic reticulum Ca^{2+} pump of skinned fibres from frog skeletal muscle. *Pflügers Arch.* 429:169–175.

Dulhunty, A. F. 1992. The voltage-activation of contraction in skeletal muscle. *Prog. Biophys. Mol. Biol.* 57:181–223.

Duty, S., and D. G. Allen. 1994. The distribution of intracellular calcium concentration in isolated single fibres of mouse skeletal muscle during fatiguing stimulation. *Pflügers Arch.* 427:102–109.

Endo, M. 1977. Calcium release from the sarcoplasmic reticulum, *Physiol. Rev.* 57:71–108.

Endo, M., and M. Iino. 1988. Measurement of Ca^{2+} release in skinned fibres from skeletal muscle. *Methods Enzymol.* 157:12–26.

Fabiato, A., and F. Fabiato. 1979. Calculator programs for computing the composition of the solutions containing multiple metals and ligands used for experiments in skinned muscle cells. *J. Physiol. (Paris).* 75:463–505.

Fink, R. H. A., and D. G. Stephenson. 1987. Ca^{2+}-movements in muscle modulated by the state of K^{+}-channels in the sarcoplasmic reticulum membrane. *Pflügers Arch.* 409:374–380.

Fink, R. H. A., D. G. Stephenson, and D. A. Williams. 1986. Potassium and ionic strength effects on the isometric force of skinned twitch muscle fibres of the rat and toad. *J. Physiol. (Lond.).* 370:317–337.

Fink, R. H. A., and C. Veigel. 1996. Calcium uptake and release modulated by counter-ion conductances in the sarcoplasmic reticulum of skeletal muscle. *Acta Physiol. Scand.* 156:387–396.

Gillis, J. M. 1985. Relaxation of vertebrate skeletal muscle. A synthesis of the biochemical and physiological approaches. *Biochim. Biophys. Acta.* 811:97–145.

Gillis, J. M., D. Thomason, J. Lefevre, and R. H. Kretsinger. 1982. Parvalbumins and muscle relaxation: a computer simulation study. *J. Muscle Res. Cell Motil.* 3:377–398.

Godt, R. E., and B. D. Lindley. 1982. Influence of temperature upon contractile activation and isometric force production in mechanically skinned fibres of the frog. *J. Gen. Physiol.* 80:279–297.

Grynkiewicz, G., M. Poenie, and R. Y. Tsien. 1985. A new generation of Ca^{2+} indicators with greatly improved fluorescence properties. *J. Biol. Chem.* 260:3440–3450.

Kargacin, G. 1994. Calcium signaling in restricted diffusion spaces. *Biophys. J.* 67:262–272.

Lamb, G. D., G. S. Posterino, and D. G. Stephenson. 1994. Effects of heparin on excitation-contraction coupling in skeletal muscle of toad and rat. *J. Physiol. (Lond.).* 474:319–329.

Lamb, G. D., and D. G. Stephenson. 1990. Calcium release in skinned muscle fibres of the toad by transverse tubule depolarization or by direct stimulation. *J. Physiol. (Lond.).* 423:495–517.

Lüttgau, H. Ch., and D. G. Stephenson. 1986. Ion movements in skeletal muscle in relation to the activation of concentration. *In* Physiology of Membrane Disorders. T. E. Andreoli, J. T. Hoffman, and D. D. Janestil, editors. Plenum Press, New York. 449–468.

MacLennan, D. H., and P. T. S. Wong. 1971. Isolation of a calcium sequestering protein from sarcoplasmic reticulum. *Proc. Natl. Acad. Sci. USA.* 68:1231–1235.

Makabe, M., O. Werner, and R. H. A. Fink. 1996. The contribution of the sarcoplasmic reticulum Ca^{2+}-transport ATPase to caffeine-induced Ca^{2+}-transients in skinned skeletal muscle fibres. *Pflügers Arch.* 432: 717–726.

Melzer, W., A. Herrmann-Frank, and H. Ch. Lüttgau. 1995. The role of Ca^{2+} ions in excitation-contraction coupling of skeletal muscle fibres. *Biochim. Biophys. Acta.* 1241:59–116.

Pape, P. C., D. S. Jong, and W. K. Chandler. 1995. Calcium release and its voltage dependence in frog cut muscle fibres equilibrated with 20 mM EGTA. *J. Gen. Physiol.* 106:259–336.

Robertson, S. P., J. D. Johnson, and J. D. Potter. 1981. The time-course of Ca^{2+} exchange with calmodulin, troponin, parvalbumin, and myosin in response to transient increases in Ca^{2+}. *Biophys. J.* 34:554–569.

Rüegg, J. C. 1996. Muscle contraction: molecular and cellular physiology. *In* Comprehensive Human Physiology, Vol. 1. Springer Verlag, New York. 935–957.

Shirokova, N., and E. Rios. 1996. Activation of Ca^{2+} release by caffeine and voltage in frog skeletal muscle. *J. Physiol. (Lond.).* 493.2:317–339.

Smith, G. D., J. Wagner, and J. Keizer. 1996. Validity of the rapid buffering approximation near a point source of calcium ions. *Biophys. J.* 70:2527–2539.

Steele, D. S., A. M. McAinsh, and G. L. Smith. 1996. Comparative effects of inorganic phosphate and oxalate on uptake and release of Ca^{2+} by the sarcoplasmic reticulum in saponin skinned rat cardiac trabeculae. *J. Physiol. (Lond.).* 490.3:565–576.

Stephenson, E. W. 1985. Excitation of skinned muscle fibres by imposed ion gradients. *J. Gen. Physiol.* 86:813–852.

Stienen, G. J. M., R. Zaremba, and G. Elzinga. 1995. ATP utilization for calcium uptake and force production in skinned muscle fibres of *Xenopus laevis*. *J. Physiol. (Lond.).* 482.1:109–122.

Uttenweiler, D., C. Weber, and R. H. A. Fink. 1997a. Ca^{2+}-movement in skinned fibres studied with fluorescence imaging and numerical modelling. *J. Muscle Res. Cell Motil.* 18:192 (Abstr.).

Uttenweiler, D., C. Weber, and R. H. A. Fink. 1997b. Numerical simulation and image analysis of the Ca^{2+}-turnover in skinned skeletal muscle fibres. *Biophys. J.* 72:A275 (Abstr.).

Uttenweiler, D., R. Wojciechowski, M. Makabe, C. Veigel, and R. H. A. Fink. 1995. Combined analysis of intracellular calcium with dual excitation fluorescence photometry and imaging. *Optical Eng.* 34:2864–2871.

Veigel, C., R. Wiegand-Steubing, A. Harim, C. Weber, K. O. Greulich, and R. H. A. Fink. 1994. New cell biological applications of the laser microbeam technique: the microdissection and skinning of muscle fibres and the perforation and fusion of sarcolemma vesicles. *Eur. J. Cell Biol.* 63:140–148.

Wagner, J., and J. Keizer. 1994. Effects of rapid buffers on Ca^{2+} diffusion and Ca^{2+} oscillations. *Biophys. J.* 67:447–456.

Zhao, M., S. Hollingworth, and S. M. Baylor. 1996. Properties of tri- and tetracarboxylate Ca^{2+} indicators in frog skeletal mucle fibres. *Biophys. J.* 70:896–916.